Journal of Modern Optics
Publication details, including instructions for authors and subscription information:
http://www.tandfonline.com/loi/tmop20

Single-mode 780 nm vertical-cavity surface-emitting lasers with multi-leaf holey tructure

Hung-Pin D. Yang [a], Jui-Nung Liu [b], Zao-En Yeh [b], Fang-I Lai [b], Tsin-Dong Lee [c], Hao-Chung Kuo [b] & Jim Y. Chi [a]

[a] Nanophotonic Center, Industrial Technology Research Institute, Chutung 310, Hsinchu, Taiwan

[b] Institute of Electro-Optical Engineering, National Chiao Tung University, 1001 Ta Hsueh Road, Hsinchu 30050, Taiwan

[c] National Yulin University of Science and Technology, Yulin 64002, Taiwan

Published online: 06 Dec 2007.

To cite this article: Hung-Pin D. Yang, Jui-Nung Liu, Zao-En Yeh, Fang-I Lai, Tsin-Dong Lee, Hao-Chung Kuo & Jim Y. Chi (2008) Single-mode 780 nm vertical-cavity surface-emitting lasers with multi-leaf holey tructure, Journal of Modern Optics, 55:2, 341-349, DOI: 10.1080/09500340701439560

To link to this article: http://dx.doi.org/10.1080/09500340701439560

Journal of Modern Optics
Vol. 55, No. 2, 20 January 2008, 341–349

Taylor & Francis
Taylor & Francis Group

LETTER

Single-mode 780 nm vertical-cavity surface-emitting lasers with multi-leaf holey structure

Hung-Pin D. Yang[a]*, Jui-Nung Liu[b], Zao-En Yeh[b], Fang-I Lai[b], Tsin-Dong Lee[c], Hao-Chung Kuo[b] and Jim Y. Chi[a]

[a]*Nanophotonic Center, Industrial Technology Research Institute, Chutung 310, Hsinchu, Taiwan;* [b]*Institute of Electro-Optical Engineering, National Chiao Tung University, 1001 Ta Hsueh Road, Hsinchu 30050, Taiwan;* [c]*National Yulin University of Science and Technology, Yulin 64002, Taiwan*

(*Received 13 March 2007; final version received 3 May 2007*)

A single-mode oxide-confined vertical-cavity surface-emitting laser (VCSEL) with multi-leaf holey structure for fiber-optic applications is demonstrated. The optical confinement was done by a multi-leaf holey structure. The deep etched leaf holes were used to provide better mode confinement and suppression of higher order modes. Single fundamental mode continuous-wave output power of over 1.1 mW has been achieved in the 780 nm range, with a threshold current of approximately 0.9 mA. Side-mode suppression ratio (SMSR) larger than 24 dB has been measured.

1. Introduction

Vertical-cavity surface-emitting lasers (VCSELs) have attracted a lot of attention in recent years. Single-mode VCSELs are needed for a number of applications, including high-speed laser printing, optical storage, and long-wavelength telecommunications. For oxide-confined VCSELs, the current-confined aperture must be less than 3 μm in diameter to ensure stable single-mode operation (*1*). However, the large resistance inherited from the small aperture limits the modulation bandwidth and degrades the high-speed performance. The lifetime of the oxide VCSEL also decreases proportionally to the diameter of the oxide aperture, even when the device is operated at a reduced current. Techniques used to solve the problem include the increase of higher order mode loss by surface-relief etching (*2*) and hybrid oxide-implanted VCSELs (*3*). Recently, a two-dimensional photonic crystal (2-D PhC) structure formed on the VCSEL surface was used as a control method of the

*Corresponding author. Email: hpyang@itri.org.tw

ISSN 0950–0340 print/ISSN 1362–3044 online

DOI: 10.1080/09500340701439560
http://www.informaworld.com

lateral mode. Single-mode output was realized from larger aperture photonic crystal VCSELs (PhC-VCSELs) (*4*). Also, single-mode VCSELs can be realized by using a triangular holey structure, combined with an oxide layer and proton implantation for current confinement in the 850 nm range (*5, 6*). The confinement of the laser output beam depends critically on the dimensions of the holey structure. Moreover, single-mode oxide-confined 780 nm VCSELs have been demonstrated (*7*). However, the small oxide aperture single-mode 780 nm VCSELs may encounter similar reliability problems as the single-mode 850 nm VCSELs (*1*). The implementation holey structure within the VCSEL is becoming an alternative approach for single-mode laser output generation. Single-mode operation of the 780 nm holey VCSEL with larger oxide aperture size is still yet to be realized. In this paper, we report our results on the oxide-confined VCSELs with multi-leaf holey structure in the 780 nm range. Multi-leaf holey structure was formed within the device for optical confinement to achieve single-mode operation. Compared to the surface relief (etching depth $\sim$ few tens to few hundred nanometers) (*8*) and photonic crystal VCSELs, the deep etched multi-leaf holey structure was used for higher-order mode suppression, where stronger mode selectivity was implemented. The photonic crystal structure provides weaker index guiding (refractive index reduction $\Delta n \sim 10^{-2}$) for the lasing output (*9*). Although similar to the air holes of the photonic crystal structure, the multi-leaf holey structure made with larger trapezoid-shaped etched holes can provide better air/semiconductor index guiding for the lasing mode at the center and loss mechanism for higher-order modes. The optical loss is larger within the etched leaf hole region because the reflectivity of the etched top distributed Bragg reflector (DBR) is greatly reduced. Higher-order modes therefore will not lase in the etched leaf hole region. Single-transverse-mode operation with side-mode suppression ratio (SMSR) of over 24 dB is demonstrated for the 780 nm holey VCSEL.

2. Experiments

The schematic of the device structure is shown in Figure 1. The eight-leaf holey structure consists of eight evenly spaced trapezoid-shaped etched holes within the p-ohmic contact ring. The radius (R) of the central laser-emitting area surrounded by the multi-leaf holes is 3.5 to 4 μm. The multi-leaf holey structure made with smaller central laser-emitting area ($R \leq 3$ μm) and larger etched holes may induce larger optical scattering loss because of possible larger laser beam size at higher currents. Compared to the previously reported triangular-shaped holey VCSELs ($R = 3$ μm) (*5*), the trapezoid-shaped holey structure in this work has a larger central laser-emitting area, which may allow higher output power emission. The effectiveness of the mode confinement is comparable. The inner and outer widths (W_1 and W_2) of the trapezoid leaf hole are 1.5 and 4 μm, respectively. The length (L_1) of the trapezoid leaf hole is 5.5 μm. The width of the unetched area between trapezoid leaf holes is 1.6 to 3.6 μm. The unetched top DBR area between the leaf holes is used for current conduction so that current can flow toward the central laser-emitting area. The possibility of emergence of higher order modes in the unetched area is greatly reduced because the unetched area between leaf holes is too small for higher order modes to occur. Even smaller width (less than 1 μm) of the unetched area will result in larger series

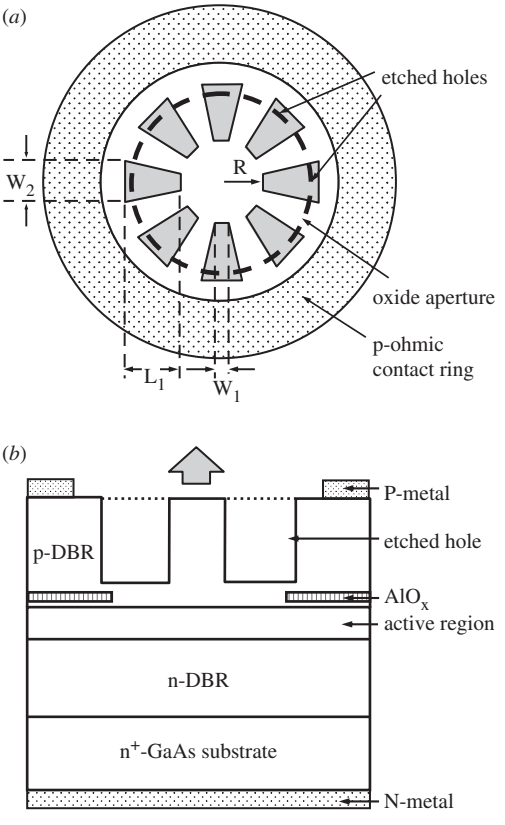

Figure 1. Schematic of the multi-leaf holey VCSEL. The inner radius (R) of the laser-emitting area is 3.5 to 4 μm. The etching depth of holey structure is 27-pair out of the 33-pair top DBR being etched off.

resistance such that the current flow toward the central laser-emitting area is reduced. The size of oxide aperture is larger than that of the central laser-emitting area. The etching depth of the holey structure is 27-pair out of the 33-pair top DBR being etched off. The epitaxial layers of the multi-leaf holey VCSEL wafers were grown on n^+-GaAs substrates by metal-organic chemical vapor deposition (MOCVD). The bottom DBR consists of a 40.5-pair n-type (Si-doped) quarter-wave stack ($\lambda/4$) of $Al_{0.9}Ga_{0.1}As$ / $Al_{0.3}Ga_{0.7}As$. The top DBR consists of 33-period p-type (carbon-doped) $Al_{0.9}Ga_{0.1}As$ / $Al_{0.3}Ga_{0.7}As$ quarter-wave stack. Higher Al-content $\lambda/4$ $Al_{0.3}Ga_{0.7}As$ layers were used as the high refractivity index material of the DBRs to avoid absorption of the lasing output in the 780 nm range. A heavily doped p-type (carbon-doped) contact layer was grown on top of the p-type DBR to facilitate ohmic contact. The graded index separate confinement (GRINSCH) active region contains three undoped $Al_{0.12}Ga_{0.88}As$ / $Al_{0.3}Ga_{0.7}As$ quantum wells (QWs). The current confinement of the device was done by the selectively oxidized AlO_x layer. Mesas with diameters varied from 48 to 52 μm were defined by reactive ion etch (RIE). The $Al_{0.98}Ga_{0.02}As$ layer within the $Al_{0.9}Ga_{0.1}As$ confinement layers was selectively oxidized to AlO_x. The oxide aperture varied from 18 to 22 μm in diameter. The p-ohmic contact ring

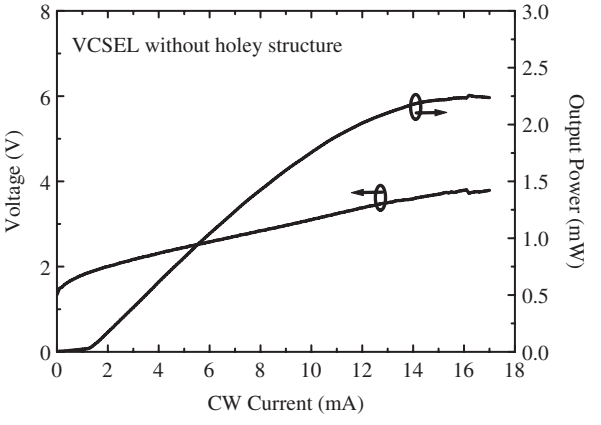

Figure 2. L–I–V characteristics of the VCSEL without holey structure. The oxide aperture of the device is 18 μm in diameter.

was formed on the top surface of the p-type contact layer. The n-ohmic contact was evaporated on the bottom surface of the n^+-GaAs substrate. The multi-leaf holey pattern was defined within the p-ohmic contact ring using photo-lithography and etched through the p-type DBR using RIE. The etching depth of holey structure is 27-pair out of the 33-pair top DBR being etched off. The actual dimension of the leaf holes was found to be slightly larger than the designed ones because of a deeper RIE etch. The almost vertically etched leaf holes done by RIE (shown in Figure 1(*b*) schematically) are suitable for lateral mode control. Using two types of apertures in this device, we decouple the effects of current confinement from the optical confinement. The AlO_x oxide aperture is used for current confinement, while the multi-leaf holey structure (with central laser-emitting area = 7 to 8 μm in diameter) within the p-ohmic contact ring is for optical confinement. In order to clarify the effect of the multi-leaf holey structure, oxide-confined VCSELs (oxide aperture = 18 to 22 μm in diameter) without holey structure were also fabricated for comparison.

3. Results and discussion

Figure 2 shows CW light–current–voltage (L–I–V) characteristics of the VCSEL without holey structure. The oxide aperture of the device is 18 μm in diameter. The threshold current (I_{th}) is 1.2 mA, with a maximum output power of 2.3 mW. The converted threshold current density (J_{th}) is 472 A cm^{-2}. The differential series resistance is approximately 150 Ω at 4 mA. Figure 3 shows CW L–I–V characteristics and near-field image at 3 mA (inset) of the eight-leaf holey VCSEL. The radius (R) of the central unetched area is 4 μm. The holey VCSEL emits 1.1 mW maximum power at 10 mA and exhibits single mode characteristics throughout the current operating range. The maximum output power of the holey VCSEL is approximately one half the maximum output power (2.3 mW) of the VCSEL without holey structure, which is because of the smaller laser-emitting area of the device. The *I*th of

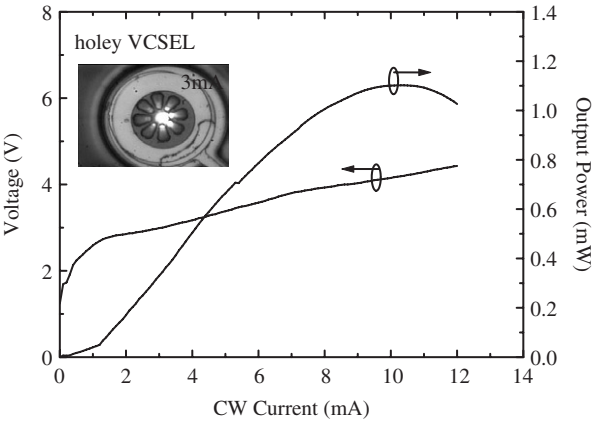

Figure 3. L–I–V characteristics and near-field image at 3 mA (inset) of the VCSEL with eight-leaf holey structure. The inner radius (R) of the laser-emitting area is 4 μm. The oxide aperture of the device is also 18 μm in diameter.

the holey VCSEL is approximately 0.9 mA. The I–V characteristics exhibit slightly higher series resistance for the holey VCSEL, which should be mainly due to partly blocking of the current flow in the device aperture region (within the p-ohmic contact ring) by etched leaf holes. The differential series resistance of the holey structure VCSEL is 200 Ω at 4 mA. Figure 4(*a*) and (*b*) show the near-field images of the eight-leaf holey VCSEL at 2 ($\sim 2.2 \times I$th) and 5 mA ($\sim 5.6 \times I$th), respectively. The near-field images were taken by a near-field imaging system with additional light illumination on the device to clearly show the holey structure of the device. The rounded lasing spot of the device is the fundamental transverse mode (TEM_{00}) at the central laser-emitting area. As shown in Figure 4(*b*), the lasing spot remains as the fundamental TEM_{00} mode at a higher current of 5 mA. The lasing spot is approximately 5.7 μm in diameter. The diameter of the central laser-emitting area (7 to 8 μm) is larger than the size of the lasing spot. A larger central laser-emitting area (with diameter greater than 10 μm) may induce multiple transverse mode lasing. The lasing area of the TEM_{00} mode slightly increased with increasing current. Some scattered lights were observed emitting out of the etched holes, which is mainly because of the greatly reduced reflectance of the etched leaf hole region. These scattered lights were originated from the TEM_{00} mode at the center, as most of the scattered lights were emitting from edges of the leaf holes close to the center. Such scattered light can be reduced with better alignment of the holey structure and the oxide aperture. Also shown in Figure 4, the resulting holey structure is slightly different from the original design in Figure 1. This is mainly because of a deep hole etching process by RIE, which is needed for better mode confinement. The slightly larger etch holes may induce more scattered light and slightly larger series resistance of the device. As compared to that of the 850 nm VCSEL (refractive index difference $\Delta n \sim 0.44$), the thickness of the top DBR of the 780 nm is larger because of the smaller refractive index difference ($\Delta n = 0.33$) between $Al_{0.9}Ga_{0.1}As$ (lower refractive index material, refractive index $n = 3.0$) and $Al_{0.3}Ga_{0.7}As$ DBR layers (higher refractive index material, $n = 3.33$). For a better mode control of the device, the multi-leaf holey structure needs to be as close to the active region of the

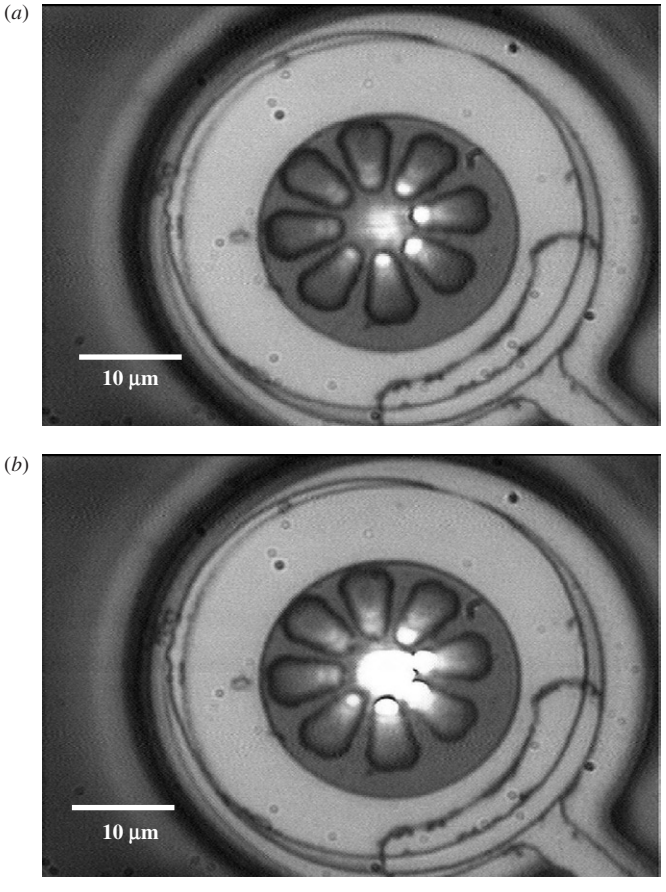

Figure 4. Near-field images at (*a*) 2 mA and (*b*) 5 mA of the VCSEL with holey structure. The inner radius (*R*) of the laser-emitting area is 4 μm.

VCSEL as possible. A deeper holey structure (etching depth $\sim$ 3.3 μm) is therefore preferred for the 780 nm holey VCSELs. Lasing spectra of the VCSEL without holey structure at 6 and 10 mA is shown in Figure 5(*a*). The spectral resolution of the optical spectrum analyzer (OSA) is 0.05 nm. The VCSEL without holey structure shows multiple transverse mode characteristics with a broader wavelength span from 776 to 780 nm and 777 to 782 nm for an injection current at 6 and 10 mA, respectively. The device showed multiple transverse mode characteristics throughout the current range. The current-dependent peak wavelength of the VCSEL without holey structure is shown in Figure 5(*b*). Since the spectra of the device has multiple emission peaks (shown in Figure 5(*a*)), the peak wavelength here (for estimation) is taken to be the emission peak with highest relative intensity in order to show the trend of lasing wavelength with injection current. The peak wavelength of the VCSEL increases from 777.9 nm at 4 mA to 780 nm at 10 mA. The increase rate of the peak lasing wavelength with current is approximately 0.4 nm mA^{-1}. Lasing spectra of the holey VCSEL are shown in Figure 6(*a*), confirming single-mode operation within the current

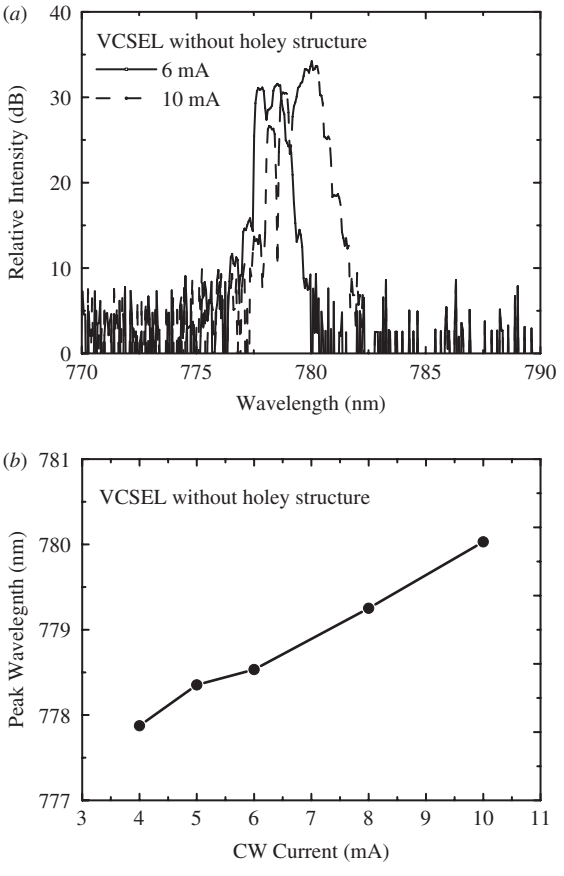

Figure 5. (*a*) Spectra at 6 and 10 mA and (*b*) current-dependent peak wavelength of the VCSEL without holey structure.

operating range. In Figure 6(*a*), the peak lasing wavelengths are 778.8 and 781.8 nm at 3 and 8 mA, respectively. The spectral bandwidth of the laser emission is much narrower than the multiple mode spectra in Figure 5(*a*). The side-mode suppression ratio (SMSR) is greater than 24 dB. No side-mode was observed within the measurement current range. These spectra results indicate that the rounded lasing spot in Figure 4(*b*) is truly TEM_{00} mode. The spectra results in Figure 6(*a*) clearly show good side-mode suppression with holey structure, where all transverse side modes are suppressed. The scattered light emitting from leaf holes does not affect the single-mode characteristics of the device. The near-field images in Figure 4 also show that the lasing mode of the device is well confined within the central laser-emitting area surrounded by the multi-leaf holey structure. Our multi-leaf holey structure, which is different from the previous studies (*5, 6*) made with smaller triangular holes, can generate comparable effects for higher order mode suppression. The larger oxide aperture (18 to 22 μm in diameter) single-mode holey VCSEL in this study is expected to be more reliable (with differential series resistance ~200 Ω) than the previously reported single-mode oxide-confined VCSEL with smaller

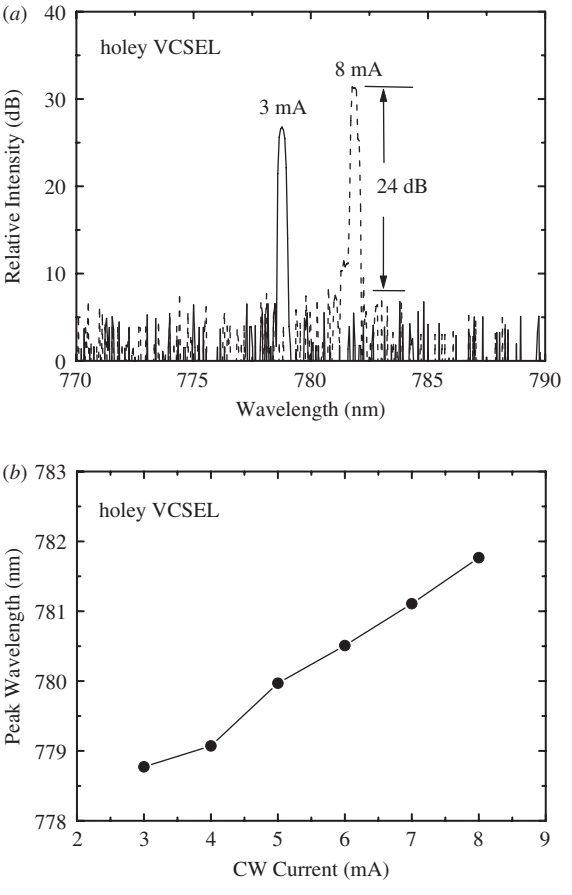

Figure 6. (*a*) Spectra at 2 and 5 mA and (*b*) current-dependent peak wavelength of the eight-leaf holey VCSELs.

oxide aperture (3.5 μm in diameter) (*1, 7*). Similar to that of the PhC-VCSELs (etching depth ~2.2 μm), a deep etching depth (27-pair out of the 33-pair top DBR being etched off) of the multi-leaf holey structure was needed (*4*). Figure 6(*b*) shows the current-dependent peak wavelength of the holey VCSEL. The peak wavelength increases monotonically from 778.8 nm at 3 mA to 781.8 nm at 8 mA. The increase rate of the peak lasing wavelength with current is approximately 0.6 nm mA^{-1}.

4. Conclusion

In conclusion, we report a single-mode 780 nm multi-leaf holey VCSEL with SMSR > 24 dB throughout the current operating range. The present results indicate that a VCSEL using an oxide layer for current confinement and a multi-leaf holey

structure for optical confinement is a promising approach to achieve single-mode operation of VCSEL. By adjusting the etching depth and dimensions of the holey structure for better mode confinement, the multi-leaf holey structure is applicable to the single-mode 780 nm VCSEL and possibly to longer wavelength VCSELs in the future.

References

(1) Hawkins, B.M.; Hawthorne, R.A., III; Guenter, J.K.; Tatum, J.A.; Biard, J.R. Reliability of various size oxide aperture VCSELs. *Proceedings of the 52nd Electron. Comps. & Technology Conference*, San Diego, CA, 28–30 May, **2002**. pp. 540–550.
(2) Haglund, A.A.; Gustavsson, J.S.; Vukusić, J.; Modh, P.; Larsson, A. *IEEE Photonics Technol. Lett*. **2004**, *16*, 368–370.
(3) Young, E.W.; Choquette K.D.; Chuang, S.L.; Geib, K.M.; Fischer, A.J.; Allerman, A.A. *IEEE Photonics Technol. Lett*. **2001**, *13*, 927–929.
(4) Yokouchi, N.; Danner, A.J.; Choquette, K.D. *Appl. Phys. Lett*. **2003**, *82*, 1344–1346.
(5) Furukawa, A.; Sasaki, S.; Hoshi, M.; Matsuzono, A.; Moritoh, K.; Baba, Y. *Appl. Phys. Lett*. **2004**, *85*, 5161–5164.
(6) Leisher, P.O.; Danner, A.J.; Raftery, J.J., Jr; Choquette, K.D. *Electron. Lett*. **2005**, *41*, 1010–1011.
(7) Ueki, N.; Sakamoto, A.; Nakamura, T.; Nakayama, H.; Sakurai, J.; Otoma, H.; Miyamoto, Y.; Yoshikawa, M.; Fuse, M. *IEEE Photonics Technol. Lett*. **1999**, *11*, 1539–1541.
(8) Söderberg, E.; Gustavsson, J.S.; Modh, P.; Larsson, A.; Zhang, Z.; Berggren, J.; Hammar, M. *IEEE Photonics Technol. Lett*. **2007**, *19*, 327–329.
(9) Yokouchi, N.; Danner, A.J.; Choquette, K.D. *Appl. Phys. Lett*. **2003**, *82*, 3608–3610.